

# Classification of $g$ -modes for neutron stars with a strong transition: Novel universal relation including slow stable twin stars

M. C. Rodríguez,<sup>1,2</sup> José C. Jiménez,<sup>3,4</sup> and Ignacio F. Ranea-Sandoval<sup>1,2</sup>

<sup>1</sup>*Grupo de Astrofísica de Remanentes Compactos,  
Facultad de Ciencias Astronómicas y Geofísicas, Universidad Nacional de La Plata,  
Paseo del Bosque S/N, 1900, La Plata, Argentina.*

<sup>2</sup>*CONICET, Godoy Cruz 2290, 1425, CABA, Argentina.*

<sup>3</sup>*Department of Astrophysics, Brazilian Center for Research in Physics (CBPF),  
Rua Dr. Xavier Sigaud, 150, URCA, Rio de Janeiro CEP 22210-180, RJ, Brazil*

<sup>4</sup>*Universidad Tecnológica del Perú, Arequipa - Perú*

(Dated: October 9, 2025)

We investigate the behavior of the non-radial gravity-pulsation discontinuity mode ( $g$ -mode) in hybrid compact stars with a strong first-order phase transition, which can give rise to twin-star configurations in some cases. These modes are of utmost relevance since they can be potentially excited in isolated as well as binary neutron star systems in the inspiral phase, thus allowing us to indirectly detect the presence of a deconfinement transition. In order to do this, we consider four categories of twin stars that present distinctive features in their equations of state. We employ the constant speed of sound parametrization, which accounts for a sharp phase transition between confined hadronic matter and deconfined quark matter. Then, working within the relativistic Cowling approximation to obtain the frequencies of non-radial oscillations, we find that, depending on the twin star category, the relations between  $g$ -mode frequencies and masses as well as tidal deformabilities display a highly distinct behavior across the diverse twin star categories that appear in the slow hadron-quark conversion regime. This distinct phenomenology provides smoking-gun evidence to clearly distinguish and further classify hybrid stars with a strong transition from purely hadronic stars using upcoming gravitational-wave data. In addition, we present for each of the categories studied the relation between the  $g$ -mode frequency and the normalized energy density jump. Finally, we present a novel universal relationship for the discontinuity  $g$ -mode able to encompass the four categories including long branches of slow stable twin stars and address its asteroseismological capability.

## I. INTRODUCTION

Neutron stars (NSs) are compact stellar remnants formed during core-collapse supernova events. Although these dense objects are born with extreme properties such as high rotation, magnetic fields, and temperature [1], they lose them as they get older. This allows us to make theoretical predictions by overlooking these properties when comparing them with current data, since most of the observed NSs are old, having millions of years of age. For instance, NSs suffer a quick thermal cooling at around 1 millisecond of age due to microscopic processes, such as neutrino emission [2], reaching temperatures in the order of  $T \sim \text{KeV}$ . However, the baryochemical potential,  $\mu_B$ , reaches values around 1.4 GeV, then giving us  $T/\mu_B \ll 1$ . In this sense, NSs can be considered cold stars on the nuclear scale. Under these conditions, heavy (masses  $\sim 2 M_\odot$ ) and compact NSs (radii  $\sim 12 \text{ km}$ ) are formed and observed as pulsars, mostly in binary systems.

These structural properties (masses and radii) imply baryon densities,  $n_B$ , several times larger than the nuclear saturation one,  $n_0 \sim 0.16 \text{ fm}^{-3}$ , at the core of NSs. In turn, this motivated the astrophysics community to hypothesize that at the inner core of NSs, such high densities might give rise to complex phases of nuclear matter, e.g. deconfined quark matter, only somewhat known in

phenomenological models [3–5]. Unfortunately, current terrestrial laboratories are far from being able to simultaneously reach these high-density and low-temperature conditions. For this reason, NSs are natural astrophysical laboratories that might help us to understand the nature of matter in such extreme regimes of pressure and density [4, 5].

Schematically, NSs can be thought of as being composed of three layers of nuclear matter with radically different behaviors: an inner core, an outer core, and a crust. Baryon densities in the crust are lower than  $n_0$ , so experimental data from laboratories can be used to reduce the uncertainties on the low-density regime of the NS matter equation of state (EoS). Moreover, calculations using Chiral Effective Theory (CET) have proven to be useful to constrain the EoS in such a density regime (see, e.g., Ref. [6] and references therein). This situation changes in the outer core and, despite the help provided by new observational data from mergers of NSs, there is still no general agreement on the behavior of matter for densities above  $n_0$ . This lack of knowledge becomes more drastic as density increases at the inner core of such compact objects. In order to describe matter in the depths of the inner core, several theoretical lines are being explored. One of these alternatives includes the existence of a hadron-quark phase transition (see, e.g., Refs. [4, 5, 7] and references therein), which might form the so-called hybrid star, meaning that they are composed of hadrons

in the outer region while quarks dominate the stellar core.

On the other hand, observations of the  $2 M_{\odot}$  pulsars PSR J1614-2230 [8] (later improved in Ref. [9]), PSR J0348+0432 [10] and PSR J0740+6620 [11] impose strong constraints on the NS matter EoS. Other constraints become available from gravitational-wave events, particularly useful was GW170817 and its electromagnetic counterpart [12–14], which offered valuable insights into the EoS and the internal structure of NSs by constraining the dimensionless tidal deformability,  $\Lambda$ , of these compact objects. In addition, observations from NASA’s NICER X-ray telescope [15–20] have been used to determine the masses and radii of isolated NSs. Since the number of increasingly precise measurements is growing rapidly, it is now feasible to test theoretical predictions against astrophysical observations and, in this manner, shed some light on the properties of matter under extreme conditions.

In principle, the calculation of the NS EoS should come from employing Quantum Chromodynamics (QCD), the best theory to treat strong interactions. The main key features of QCD are confinement, chiral symmetry breaking and asymptotic freedom which combined suggest that strongly interacting matter must suffer a phase transition at intermediate baryon densities/temperatures, in which hadrons liberate their internal components, i.e. quarks and gluons forming dense/hot quark matter. In particular, performing lattice QCD calculations at finite baryon densities is extremely difficult (perhaps impossible) as the theory has intrinsic computational problems coming from the so-called “fermionic sign problem” when computing thermodynamic observables with quantum Monte Carlo techniques [21, 22]. This is one of the main reasons that lead to the development of several phenomenological and effective models that could reproduce and yield a proper understanding of (at least some) key features of QCD while keeping (or breaking as with the chiral symmetry) some of its underlying symmetries (see, e.g., Refs. [4, 5] and references therein).

In this sense, one of the most challenging open questions in extreme QCD physics is connected to determining the existence and nature of a potential phase transition to deconfined quark matter at intermediate baryon densities and its possible realization at the inner core of (high-mass) NSs. Interestingly, this complex phenomenon could also leave unique imprints not only in *quasi-static* observables (e.g. masses, radii, tidal deformabilities), but also in *oscillatory* ones, such as their non-radial oscillation modes which might be excited in isolated NSs due to their internal composition or by external gravitational fields, as occurs in binary NS systems [23–25]. This opens a window with the potential to characterize the unknown microphysics tightly connected to phase transitions inside compact stars.

Currently, one intriguing possibility for this hypothesized hadron-quark phase transition at low temperatures and high densities is that it could be of first order (see, e.g., Refs. [26, 27]). If this is true, it still remains un-

known if it must be described using the Maxwell or the Gibbs thermodynamic constructions for such a type of phase transition (see, e.g., Refs. [4, 5] and references therein). The main difference between these approaches resides in the fact that along a Gibbs phase transition, the pressure and energy density (but not the speed of sound) are continuous along the mixed phase, whereas in a Maxwell phase transition at a given transitional pressure,  $P_t$ , the energy density,  $\epsilon$ , suffers a jump,  $\Delta\epsilon$ . Another difference is the fact that in the mixed phase of the Gibbs construction, charge neutrality in each volume element is attained globally and not locally as in the Maxwell case. The principal quantity that determines which of the two thermodynamic constructions is favored is the hadron-quark surface tension,  $\sigma_{\text{HQ}}$ . Values below the critical threshold, estimated to be around  $\sigma_{\text{HQ}}^{\text{crit}} \sim 5 - 40 \text{ MeV/fm}^2$  favor mixed phases, whereas larger values favor a sharp interphase (see, e.g., Ref. [28] and references therein). Unfortunately, this quantity is currently poorly constrained, and only a precise determination of  $\sigma_{\text{HQ}}$  would allow us to know the nature and properties of the hadron-quark phase transition.

Additionally, if the phase transition is sharply discontinuous, the timescale of conversion of hadrons into quarks (and vice versa) has been shown to play a key role in the dynamical stability of hybrid stars against linearized radial perturbations. Ref. [29] had shown that if the nucleation timescale is much larger than the oscillation period of the radial perturbations, then stellar configurations in a branch where  $\partial M/\partial\epsilon_c < 0$  can be dynamically stable (for a review on the subject see [28] and references therein). This is the *slow* conversion regime where the fluid elements in the vicinity of the transition surface keep their nature when stretched or compressed around the transition pressure where an extended branch of *slow stable hybrid stars* (SSHS) might appear. In the opposite case, the *rapid* regime, the standard stability criteria ( $\partial M/\partial\epsilon_c \geq 0$ ) remain valid. The *slow* transition hypothesis has been used to study astrophysical implications in several previous works [30–45]. Such studies serve to prove the robustness of the SSHS scenario independently of the nature of the hybrid EoS used.

A future area that might result relevant to NS astrophysics is the one related to detecting gravitational waves from isolated NSs (see, e.g., Refs. [46–49] and references therein). In this context, the study of the quasi-normal modes becomes of paramount importance. Particularly, cold hybrid stars have a distinctive *g*-mode associated with the discontinuity in the energy density that can be excited only if the conversion speed is *slow* (see, e.g., Ref. [32] and references therein). Several studies have put attention to this particular mode [33, 36, 50–53]. Moreover, universal relationships associated with non-radial oscillation modes, such as the *g*-mode studied here, play a key role in asteroseismology (see, the pioneering work Ref. [54], the recent review of Ref. [48] and references therein).

The general idea associated with universal relation-

ships including non-radial quasi-normal modes is to obtain (almost) EoS independent relationships between the frequency and damping times of particular eigenmodes and macroscopic quantities of the pulsating compact object. For example, in the case of the fundamental mode ( $f$ -mode), several universal relationships relate their associated frequencies with the gravitational mass,  $M$ , and the radius,  $R$  (see, e.g., Refs. [54–57]). Other ones relate the  $f$ -mode frequencies to the moment of inertia,  $I$ , (see, e.g., Refs. [57, 58]) and dimensionless tidal deformability,  $\Lambda$  [59, 60]. Of course, there exist also universal relations for the  $p$ -modes [54, 55],  $g$ -modes (associated with sharp hadron-quark phase transitions but not for long branches of SSHS as the ones of the present work) [33, 52] and also the axial and polar  $wI$ -modes [40, 55, 56, 61].

However, in spite of the enormous amount of works exploring these quasi-normal modes in hadronic, quark and hybrid stars (see, e.g., Ref. [62]), we realized that in the current literature no work has explored in full detail the  $g$ -modes inside hybrid stars nor have they proposed universal relations for this specific non-radial mode inside ultra-dense branches of SSHSs. In particular, there are no studies of this mode for the four broad categories of hybrid stars representing different properties of the strong first-order phase transition, e.g. large/intermediate values for the energy density jumps,  $\Delta\epsilon$ , or low/large values for the deconfinement transitional pressures,  $P_t$ . Related to that, it is worth mentioning that although Refs. [32, 33, 62] explored NSs with first-order discontinuities in the EoS, their stellar families assumed low values of  $\Delta\epsilon$  overlooking also the Seidov criterion to get a disconnected branch of stars before reaching the third branch sector, thus not producing twin star configurations properly in the classical [63, 64] and modern sense [65].

For all these reasons, we believe that a careful investigation of the  $g$ -modes inside hybrid stars is mandatory since it has been understood some years ago that any potentially observed hybrid star could be classified within the four categories explored in detail in Refs. [66, 67] for which one can, in principle, build universal relations for each one of them relating stellar structural and oscillatory properties to features of the hybrid EoS. In particular, the dependency of the  $g$ -mode frequencies against masses, tidal deformabilities, and radii. In fact, it was proven in Ref. [32] that these kinds of calculations for this  $g$ -mode should be done only for the SSHS, i.e. slow phase conversion dynamics allow finite computations of the associated frequencies, whereas rapid phase conversions will never produce finite values of frequency for this non-radial mode.

The main goal of this work is to study the  $g$ -mode frequencies of HSs within the relativistic Cowling approximation for the four categories, assuming that only slow phase conversions occur at the radial interface separating the hadronic and quark phases, which in turn affect the boundary conditions of the non-radial quasi-normal equations. The paper is organized as follows. In Sec. II,

we present basic theoretical aspects about the four categories of hybrid EoSs considered in this work, which are described using the constant-speed-of-sound (CSS) parametrization. Besides, we describe the non-radial perturbation equations within the relativistic Cowling approximation, adding also information about the slow junction conditions at the interface point. In Sec. III we present our findings for the behavior of the  $g$ -mode frequencies depending on the masses and tidal deformabilities. Moreover, in Sec. IV we analyze the relations between the  $g$ -mode frequency and the normalized energy density jump within each category of hybrid stars. Building on this, we then propose a novel universal relation that uniquely encompasses all four categories, including configurations with long branches of slow stable hybrid stars. Finally, Sec. V is devoted to presenting a summary of our key findings, in particular, to discuss our proposed universal relations and their astrophysical implications when future multimessenger data become available allowing us to distinguish HSs from other types of compact stars. For completeness, radial profiles of the perturbation functions for the  $g$ -modes are provided in Appendix A, while Appendix B presents the formalism used for the calculation of the dimensionless tidal deformability in NSs with a first-order phase transition.

## II. MICROPHYSICS AND QUASI-NORMAL ASTEROSEISMOLOGY

As already pointed out, in this section we explain the fundamental aspects of the physics underlying the EoS for twin star matter for the four categories, as well as how these aspects enter the non-radial oscillation equations when determining the oscillation frequencies of the  $g$ -mode within the relativistic Cowling approximation. Notice that although in Subsec. II A we work with physical units when defining the range of validity of each EoS, whereas in Subsec. II B and in the Appendices we adopt geometrical units ( $G = c = 1$ ) for simplicity.

### A. Hybrid equations of state

Since its inception some decades ago (see Ref. [63]), the EoSs employed to obtain twin star configurations considered a matching between a hadronic and a quark matter EoS. The aforementioned matching could be done by applying the Maxwell (with no mixed phase [65]) or the Gibbs-Glendenning (with the presence of a sizeable mixed phase [64, 68]) constructions. However, as it is still unclear which type of construction follows the QCD deconfinement transition at finite baryonic densities, one has the freedom to choose between the two possibilities. For the present work, we choose the Maxwell construc-

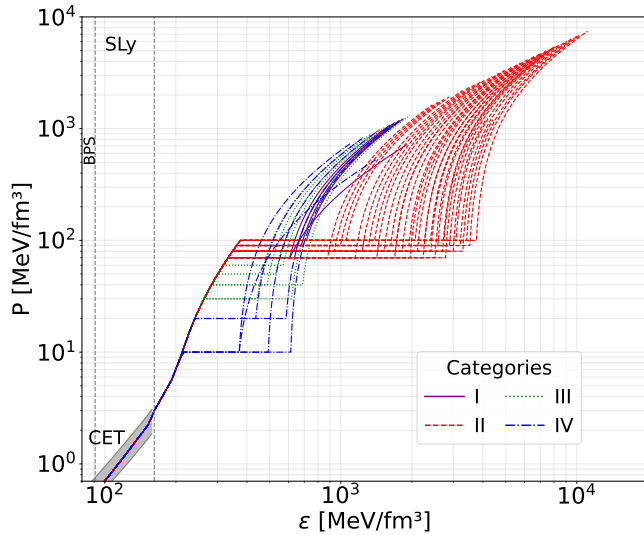


FIG. 1. Set of EoSs,  $P = P(\epsilon)$ , for hybrid matter for the four categories explored in this work. We included the region of densities for the crust, i.e. the BPS EoS, and the exterior hadronic mantle, i.e. the SLy EoS. This last SLy EoS is then smoothly matched to the EoSs at higher densities where one can classify them in different categories (labeled I-IV) meaning different physics around the transition point. Additionally, the CET band is shown at low densities illustrating the agreement of our employed hybrid EoSs with this well known first-principle hadronic EoS.

tion<sup>1</sup> since it allows a large parameter space of viable twin stars, which satisfy the classical Seidov criterion, which enforces the idea of a disconnected unstable branch after the hadronic phase, thereby giving rise to the third branch of stable stars, the so-called ultradense twin star family (see, e.g., Ref. [67]).

As already mentioned, we use the CSS parametrization for the quark sector of the hybrid EoSs [75]:

$$\epsilon(P) = \begin{cases} \epsilon_H(P) & P < P_t, \\ \epsilon_H(P_t) + \Delta\epsilon + c_s^{-2}(P - P_t) & P > P_t, \end{cases} \quad (1)$$

where  $\epsilon_H$  is the hadronic EoS dependent on the pressure until the transition point  $P_t$  before the quark phase starts above  $P_t$ . Moreover,  $\Delta\epsilon$  is the jump in the energy density and  $c_s^2$  is the squared speed of sound of the quark phase, which within this parametrization is also a free constant but which should be  $\gtrsim 0.5$  to favor *totally stable* hybrid stars (i.e. hybrid configurations that are stable both in the slow and rapid conversion scenario).

Since all the information about the quark phase is encoded in the set of parameters  $\{\Delta\epsilon, c_s^2, P_t\}$ , then we need

further information about the hadronic EoS to determine consistently the term  $\epsilon_H(P_t)$ . For this work, we use the famous Skyrme-Lyon (SLy) nuclear EoS in its tabulated version [76] for baryonic densities between  $0.5792 n_0$  and  $1.1 n_0$ . Notice that this is the same range of validity of the CET band of results for the stiff, intermediate and soft EoSs [77]. As one can see from Fig. 1, the SLy EoS lies more or less in the middle of the CET band, but it becomes stiffer at increasing densities. This is in marked contrast to past works where only the stiffer CET EoS is employed to ensure the existence of the twin star family. On the other hand, at lower baryon densities, i.e. below  $0.5792 n_0$ , we employ the Baym-Pethick-Sutherland (BPS) [78] valid until the hybrid star's surface.

After fixing the EoS for the hadronic phase up to  $n_B = 1.1 n_0$ , we point out details of the hadronic EoS at higher densities until reaching the quark phase, as displayed in Fig. 1. For the present work, we choose the EoSs from Ref. [44] which connect the hadronic and twin-star branch through an intermediate subfamily of slow stable hybrid stars, thus ensuring the dynamical stability of the whole stellar sequence. Thus, we employed three generalized piecewise polytropes (GPP) for three regions of density until the quark phase, as explained in detail in Sec. IIA of Ref. [44]. Beyond that critical pressure, we employed the same CSS parameters  $\{\Delta\epsilon, c_s^2 \sim [0.5, 1], P_t\}$  as those from Ref. [44] at the transition point for the studied SSHS in that work.

It should be noted that in Ref. [44], SSHSs were considered only in very specific cases, mainly for comparison with the rapid conversion scenario, which was the central focus of that work. Although SSHSs share similar equations of state, they appear more frequently, since they can exist in regions where fully stable HSs remain unstable. In contrast, in the present study we restrict ourselves to the slow conversion regime, as  $g$ -modes are excited exclusively under these conditions, and because Ref. [44] has already demonstrated that SSHSs are dynamically stable against radial oscillations when slow junction conditions are applied.

For completeness, in Table I, we list the extreme values of two representative EoSs for each HS category, keeping in mind that they must produce the following astrophysical features: i) Category I with the maximum masses of the hadronic and HS branches surpassing the  $2 M_\odot$  limit; ii) Category II with the maximum mass of the hadronic branch reaching the  $2 M_\odot$  value; iii) Category III with the maximum of the hadronic family lying between 1 and  $2 M_\odot$ , and the HS star branch surpassing the  $2 M_\odot$  limit; and iv) Category IV with the maximum of the hadronic branch lying below  $1 M_\odot$  while the HS branch surpasses the  $2 M_\odot$  limit.

Interestingly, one can easily verify, using the particular EoS parameters given in Table I, that, as stated in Ref. [66], the maximum values of masses reached by each branch of each category directly depend on the values taken by the triad  $\{\Delta\epsilon, c_s^2, P_t\}$ .

<sup>1</sup> There are other type of  $g$ -modes associated to the internal composition and chemical equilibrium in the Gibbs mixed phases [69–73] with recent results at finite temperatures in Ref. [74].



Category	$\Delta\epsilon$	$P_t$	$c_s^2$	$\epsilon_t$
I	274 – 340	70 – 100	0.5 – 1	333 – 374
II	545 – 3376	70 – 100	0.5 – 1	333 – 374
III	178 – 405	30 – 60	0.5 – 1	263 – 317
IV	154 – 397	10 – 20	0.5	215 – 240

TABLE I. Selected EoS parameters for each category, where  $\Delta\epsilon$  denotes the discontinuity in energy density at the transition;  $P_t$  is the transition pressure;  $c_s^2$  is the squared speed of sound, normalized to the speed of light; and  $\epsilon_t$  is the energy density at the transition. All quantities, except  $c_s^2$ , are expressed in units of MeV/fm<sup>3</sup>.

## B. Non-radial modes in the Cowling approximation

As already summarized in the Introduction, our main aim of the present work is to calculate the frequencies associated with the  $g$ -modes produced by discontinuities in the EoS coming from first-order phase transitions, which in our case are manifested as twin stars. For this, we assume that these ultra-dense compact objects possess spherical symmetry, i.e. no stationary nor differential rotation. This hypothesis allows us to use the Tolman-Oppenheimer-Volkov (TOV) equations to determine their structural features, such as masses and radii, and thereby construct the corresponding mass-radius relation to be compared with modern astronomical data.

In general, the calculation of the non-radial mode frequencies is done by studying quadrupolar perturbations considering time-dependent even-parity perturbations of the metric functions coupled to disturbances of the thermodynamic variables. This is the so-called general-relativistic linear perturbation theory [32]. Unfortunately, the numerical cost to obtain these results is quite expensive, and one usually uses a reasonable approximation called the ‘relativistic Cowling approximation’ [79], where only the fluid perturbations are considered in a fixed background space-time. Interestingly, this simplification gives quite accurate results for the oscillation frequencies when compared to the full problem (see, e.g., Refs. [57, 80] and references therein). In the particular case of the  $g$ -modes, the differences between both calculations are only of  $\sim 10\%$  [32, 50]. Unfortunately, one of the major drawbacks of this approximation is that the damping times of these quasi-normal modes cannot be obtained. In any case, given the proven reliability of this approach for determining oscillation frequencies, we also use the Cowling approximation when calculating the  $g$ -mode of SSHS. Our results capture both the qualitative and quantitative features of the full (numerically challenging) calculation, which, in some cases, may become unreliable and still require additional simplifications to clearly distinguish the  $g$ -mode from other non-radial modes with comparable values [32].

Within this approximation, we can still work with the spherically-symmetric spacetime having a line element

that can be written as

$$ds^2 = -e^{\nu(r)} dt^2 + \left(1 - \frac{2m(r)}{r}\right)^{-1} dr^2 + r^2 d\Omega^2, \quad (2)$$

where  $d\Omega^2 = d\theta^2 + \sin^2\theta d\phi^2$  is the metric on the two-sphere,  $\nu(r)$  and  $m(r)$  are the metric and mass profiles, respectively, obtained after solving the TOV equations (with appropriate boundary conditions). Notice that although the TOV equations provide solutions usually for the pressure or energy density profiles,  $P(r)$  or  $\epsilon(r)$ , one can also obtain  $\nu(r)$  from these solutions [1].

It is worth mentioning that the onset of strong transitions is (generally but not always) manifested as kinks in the  $M$ - $R$  relations, then exhibiting decreasing values of  $\{M, R\}$  for increasing central pressures ( $P_c$ ). From the hydrostatic perspective (and rapid phase-conversion viewpoint), these  $M$ - $R$  sectors close to the phase transition are often considered unstable since the values of central pressure are small compared to the magnitude of  $\Delta\epsilon$ , thus having values of  $P_c$  not enough to counter-balance such high values of corresponding central energy density. For instance, in Fig. 1, Category II EoSs have  $\Delta\epsilon \sim 3000$  MeV/fm<sup>3</sup>, while central pressures above the transition are  $P_c \sim 200$  MeV/fm<sup>3</sup>.

Following the usual procedure presented in Ref. [80], after decomposing the perturbation equations in spherical harmonics while assuming a harmonic time dependence ( $\sim e^{i\omega t}$  with  $\omega$  being the non-radial oscillation frequency), the relativistic Cowling equations governing the behavior of the fluid perturbations (characterized by functions  $V$  and  $W$ ) that need to be solved to obtain the non-radial mode oscillation frequencies are:

$$\frac{dW(r)}{dr} = \frac{d\epsilon}{dP} \left[ \omega^2 \frac{r^2}{\sqrt{1 - \frac{2m(r)}{r}}} e^{-\nu(r)} V(r) + \frac{1}{2} \frac{d\nu(r)}{dr} W(r) \right] - \frac{\ell(\ell+1)}{\sqrt{1 - \frac{2m(r)}{r}}} V(r) \quad (3)$$

and

$$\frac{dV(r)}{dr} = \frac{d\nu(r)}{dr} V(r) - \frac{1}{\sqrt{r - 2m(r)}} W(r). \quad (4)$$

In order to solve Eqs. (3)-(4), we choose  $\ell = 2$  (quadrupole oscillations) and impose boundary conditions at the stellar center ( $r \sim 0$ ), where the behavior of the solutions is [80]

$$W(r) \sim r^{\ell+1}, \quad V(r) \sim -\ell^{-1} r^\ell, \quad (5)$$

as well as at the stellar surface ( $r = R$ ) where the Lagrangian perturbation to the pressure needs to vanish,

$$\Delta P(R) = 0. \quad (6)$$

This last condition can be written as

$$\omega^2 \left[ \sqrt{1 - \frac{2M}{R}} \right]^{-\frac{3}{2}} V(R) + \frac{1}{R^2} W(R) = 0. \quad (7)$$

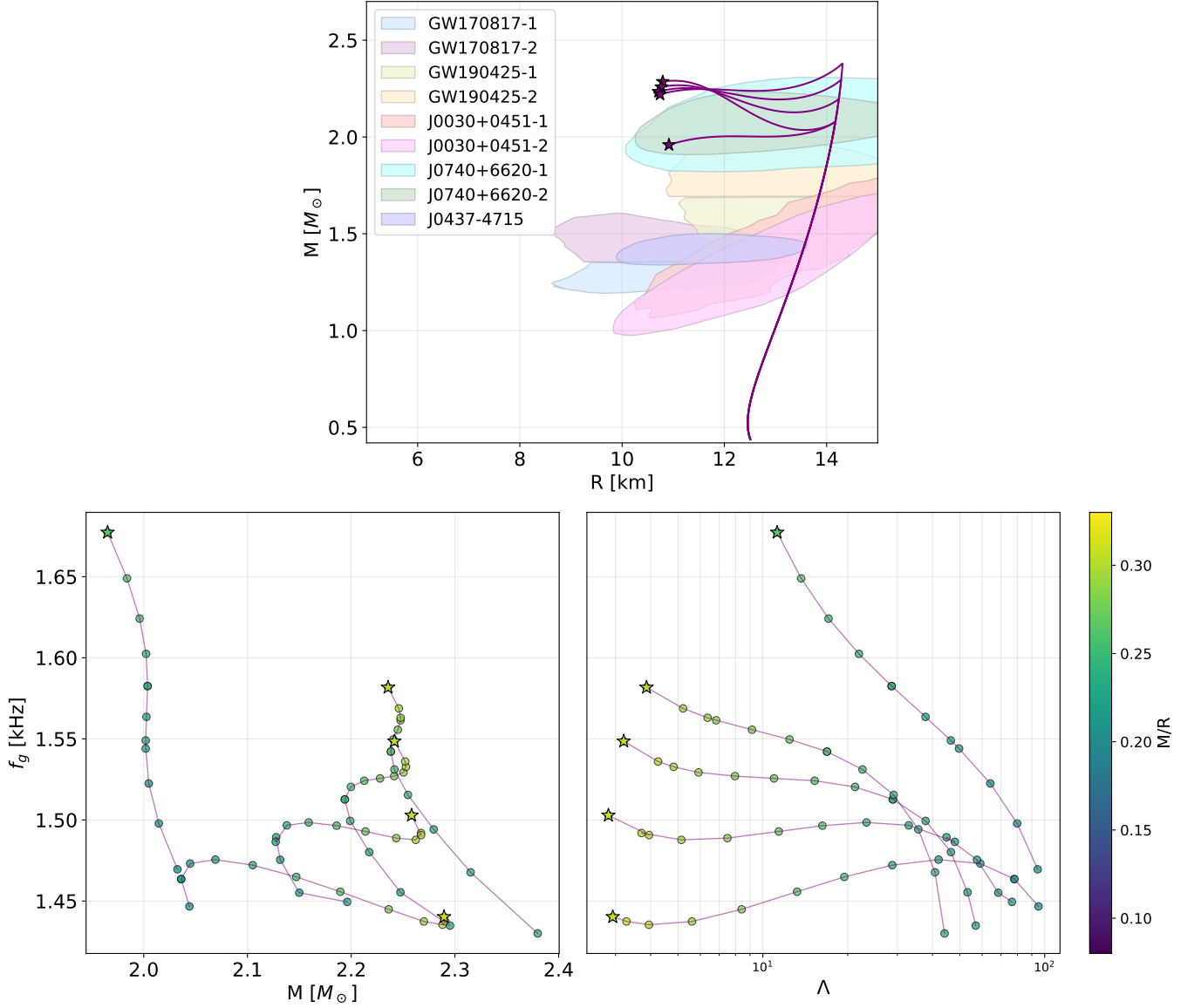


FIG. 2. Results for Category I twin stars. *Top panel:* Mass–radius relations ( $M$ - $R$ ) for hadronic and twin stars with observational constraints from NICER (PSR J0437-4715, PSR J0740+6620, and PSR J0030+0451) and gravitational wave events (GW190425 and GW170817) for comparison. *Bottom-left panel:*  $g$ -mode frequency,  $f_g$ , as a function of stellar mass,  $M$ , where the color gradient represents the compactness ( $M/R$ ) of the star. *Bottom-right panel:*  $f_g$  as a function of the dimensionless tidal deformability,  $\Lambda$ .

The values of  $\omega^2$  that satisfy Eq. (7) are the eigenfrequencies of the non-radial eigenmodes we are interested in obtaining<sup>2</sup>.

For our case of twin stars having an EoS containing a discontinuity (characterized by the  $\Delta\epsilon$  term) located at a particular radial coordinate,  $r = r_t$ , additional junction conditions at the discontinuity surface need to be

imposed:

$$W_+ = W_- , \quad (8)$$

$$V_+ = \frac{e^\nu}{\omega^2 r_t^2} \left( 1 - \frac{2m}{r_t} \right) \times \left( \frac{\epsilon_- + P}{\epsilon_+ + P} \left[ \omega^2 r_t^2 e^{-\nu} \left( 1 - \frac{2m}{r_t} \right)^{-1} V_- + \nu' W_- \right] - \nu' W_+ \right) , \quad (9)$$

<sup>2</sup> It is important to recall that Eqs. (3)-(4) together with Eq. (6), i.e. the boundary condition, conform a Sturm-Liouville problem.

where the subindex  $- (+)$  is used to characterize quantities before (after) the phase transition. It is important to note that, in the absence of discontinuities, the function  $V(r)$  becomes continuous and  $V_+ = V_-$ .

The frequencies of the  $g$ -modes are obtained using the CFK code developed in Ref. [52] which solves (given a trial frequency of a given mode  $n$ ,  $\omega_{n,\text{trial}}^2$ ) the system of Eqs. (3)-(4) using a Runge-Kutta-Fehlberg integrator. Integration is performed from the center to the transition interface, where the conditions given by Eqs. (8)-(9) are employed. Then, integration is performed up to the surface of the star, where the boundary condition given by Eq. (6) needs to be fulfilled. To solve the eigenfrequency problem we apply the root-finding algorithm which is composed of a Newton-Raphson scheme coupled with Ridder's method (see, Ref. [52] for more details on the numerical scheme used to solve this eigenvalue problem). Furthermore, the identification of these modes as  $g$ -modes is supported by the analysis of the radial profiles of the eigenfunctions  $W$  and  $V$ , as shown in Appendix A, where each eigenfunction exhibits a single node and the frequencies are found to be lower than the  $f$ -mode, consistent with the Cowling classification scheme.

### III. $g$ -MODES OF TWIN NEUTRON STARS

In this section, we display our results for the  $g$ -mode oscillation frequencies of NSs containing a strong first-order phase transition (dubbed twin stars) using four categories of EoSs for their interiors, as described in Section II A. Notice that in the top-left panels of Figs. 2-5, we show the  $M$ - $R$  relations for a particular set of EoSs within each category, along with observational constraints from the binary NS mergers GW170817 [13, 81] and GW190425 [14], as well as from NICER measurements for PSR J0740+6620 [17, 18], PSR J0030+0451 [15, 16], and PSR J0437-4715 [20]. Besides, the legends of the astrophysical constraints in the  $M$ - $R$  diagram, the labels '1' and '2' refer to the constraints derived from Ref. [17] and Ref. [18], respectively. Moreover, we stress that all our curves of results for these Figs. 2-5 represent dynamically stable configurations of hadronic and twin branches due to a detailed proof given in Ref. [44], where slow conversion dynamics and corresponding junction conditions at the transition point were assumed.

The top-right panels of Figs. 2-5 display the frequency of the  $g$ -mode,  $f_g = \omega_g/2\pi$ , as a function of the gravitational mass  $M$ , with a color gradient representing the compactness,  $M/R$ , of the star, also illustrating its influence on the  $g$ -mode frequencies. The bottom-left panels show  $f_g$  as a function of the dimensionless tidal deformability  $\Lambda$ . The star symbols in the panels indicate the terminal configuration, and in the bottom panels, their color further encodes the corresponding compactness. Results among different categories are displayed using different colors and line styles, indicating the corresponding EoS category. A global comparison among the results of these

four categories reveals distinct trends in the behavior of the  $g$ -mode frequencies, which are closely related to the properties of the transition point, e.g., large discontinuities in the energy density at the phase transition or earlier transitions to deconfined quark matter. With this in mind, one could expect quantitative and qualitative variations of  $f_g$  between categories at increasing densities after the transition occurs. Moreover, it will be easy to note that all our hybrid EoS produce stellar configurations consistent with current observational constraints from NICER and gravitational-wave data.

In the following, we present the analysis of the  $g$ -mode frequencies for each EoS category (displayed in Figs. 2-5) as follows:

- **Category I:** The results related to this category are presented in Figure 2. This family of hybrid stars (mostly twin but also triplet in our present slow conversion scenario) have frequencies,  $f_g$ , lying in the range  $\sim 1.4 - \sim 1.7$  kHz. The SSHS near the terminal configuration have cores composed by quarks with a size of about 70% of the star and with a compactness around  $M/R \sim 0.25$ . We can see that there is no generic behavior of the frequency  $f_g$  with the mass, despite in most of the cases analyzed,  $f_g$  increases as the terminal configuration is reached. A similar situation occurs when the behavior of  $f_g$  with the dimensionless tidal deformability,  $\Lambda$ , is analyzed. In general, as  $\Lambda$  decreases towards the terminal configuration,  $f_g$  increases. Despite this behavior can be thought to be generic, there are exceptions with some curves displaying non-monotonic behavior.
- **Category II:** The results related to this category are presented in Figure 3. The numerical values of frequencies  $f_g$  within this category are notably higher than those of Category I and all other categories (see also Fig. 7 below), i.e. they lie in the range  $\sim 2 - \sim 5$  kHz. This is unexpected since typical values for ordinary hybrid stars - stable under both the slow and rapid conversion scenarios - remain below  $\sim 2.5$  kHz (see, e.g., Refs. [50-52, 82] and references therein). This category corresponds to the most elongated extended branches of SSHS. Nevertheless, near the terminal configuration the quark cores generally do not exceed  $\sim 65\%$  of the stellar radius, and the compactness typically remains below  $\sim 0.25$ . For objects in this category, it becomes more evident that the frequency  $f_g$  increases along the extended stability branch toward the terminal configuration, reaching higher values for lower-mass SSHS.
- **Category III:** As can be seen from Fig. 4, the values of  $f_g$  are between  $\sim 1 - \sim 2$  kHz. We separated in the  $M$ - $R$  diagram two families with higher and lower hybrid-star masses, i.e.  $M \sim 2.4M_\odot$  and  $M \sim 2M_\odot$ , respectively. We do this for clarity in

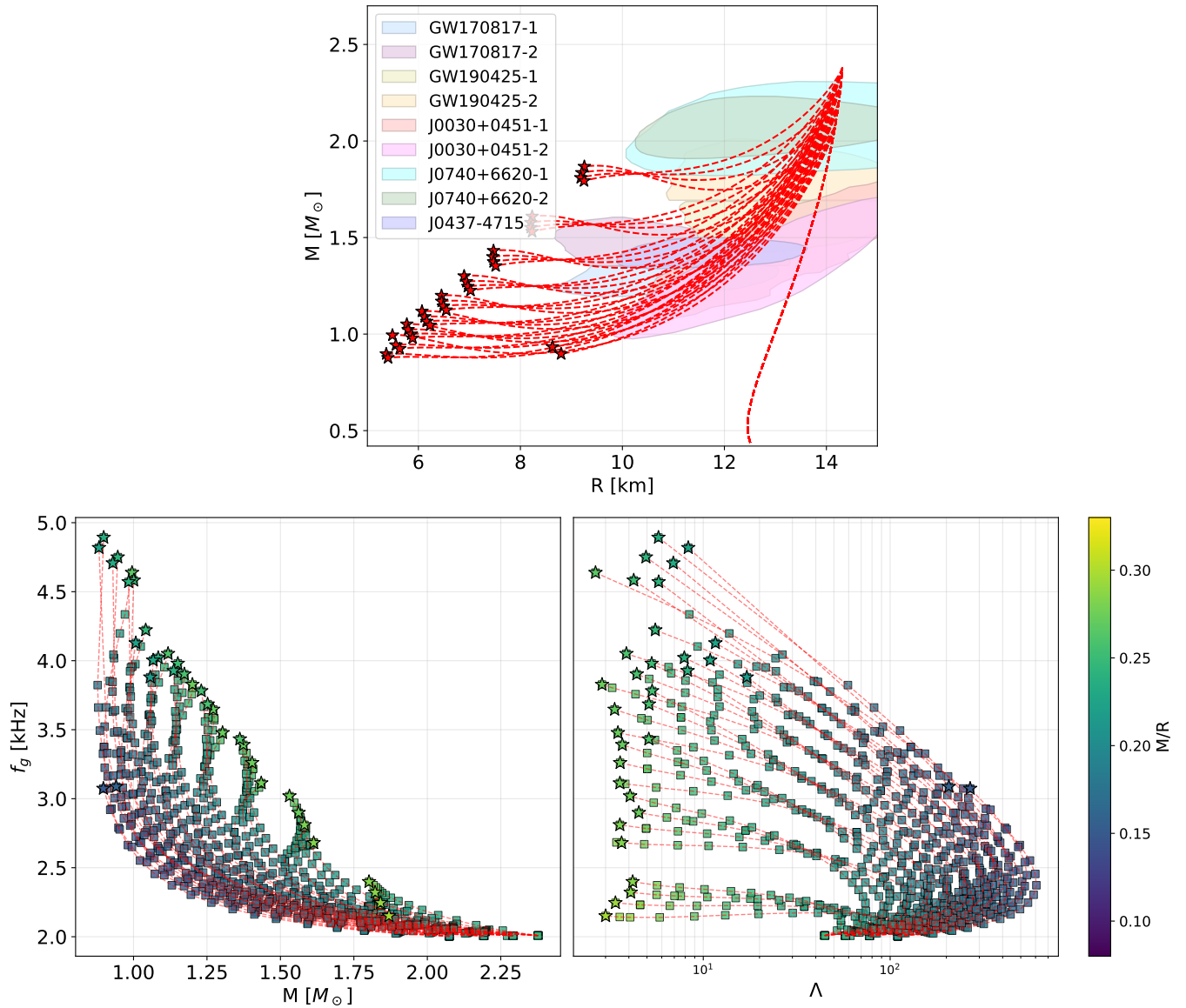


FIG. 3. Results for Category II twin stars. Same legends and astrophysical constraints as that of Fig. 2.

the presentation of our results and analysis. With that in mind, one can see in the  $f_g$ - $M$  plane that the four families that reach gravitational masses  $M \sim 2.4M_\odot$  have lower  $f_g$  compared to the two lower-mass ( $M \sim 2M_\odot$ ) families.

For this category, the general behavior of  $f_g$  is that it decreases with the mass of the HS. Moreover, for this families, no long branches of SSHS appear after the maximum mass configuration where the quark core occupies more than 80% of the star. Despite this fact, it is important to remark that triplets are possible as SSHS that connect the hadronic branch with the *totally stable*<sup>3</sup> branch of HS appear af-

ter the phase transition takes place. As a function of the dimensionless tidal deformability  $\Lambda$ , the frequency  $f_g$  decreases almost monotonically: the more compact objects in this category exhibit both lower  $\Lambda$  and lower  $f_g$  than the first HSs formed after the phase transition.

- **Category IV:** As can be seen from Fig. 5, the  $g$ -mode frequencies lie in the range 0.7–2.1 kHz. Despite having transition pressures lower than those of Category III, the general behavior of  $f_g$  with the mass and dimensionless tidal deformability are

<sup>3</sup> Hybrid configurations that are stable both in the slow and rapid

regime of conversion between phases.



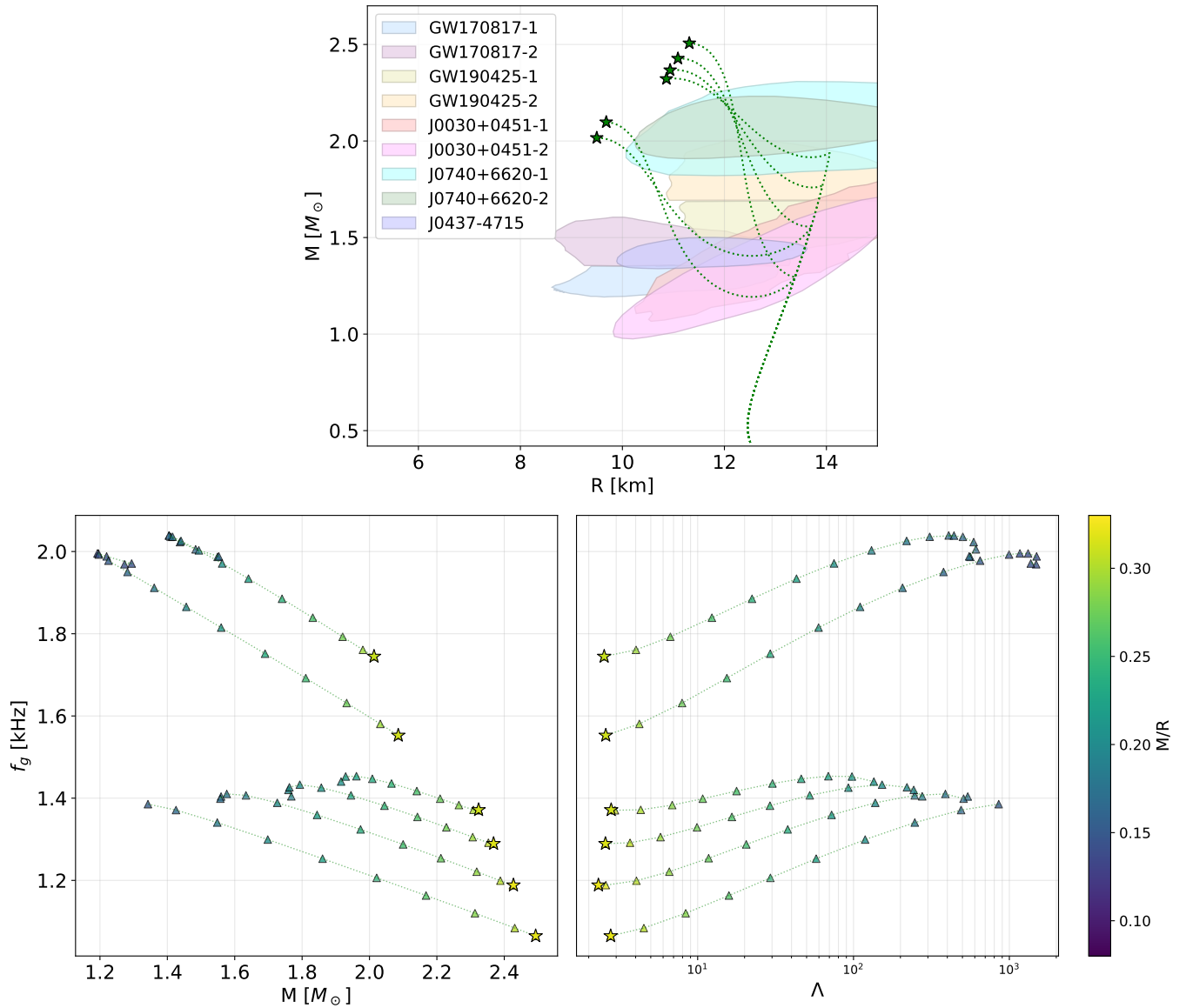


FIG. 4. Results for Category III twin stars. Same legends and astrophysical constraints as that of Fig. 2.

qualitatively similar. The larger deviations between both categories can be seen for extremely low-mass HSs where  $f_g$  decreases with the mass but increases with  $\Lambda$  until the behavior described previously towards the terminal configuration (where compactness is larger than 0.3 and the quark core represents  $\sim 85\%$  of the stellar configuration) is regained. As in Category II, triplets of low mass ( $M < 1 M_\odot$ ) are possible but no SSHS appear after the maximum mass configuration is reached.

In addition, it is relevant to analyze the behavior of the tidal deformability as a function of the stellar mass. In Fig. 6, we display  $\Lambda(M)$  for all four categories of HSs considered in this work. The same color code as in previous figures is used to distinguish between categories,

while the black star (with the error bars) corresponds to the constraint on the tidal deformability of a  $1.4 M_\odot$  NS reported in Ref. [83]. We note that not all equations of state within each category satisfy this constraint. For Category I, we note that no SSHS configurations were obtained around  $1.4 M_\odot$ ,  $\Lambda_{1.4}$ , and therefore the  $\Lambda_{1.4}$  constraint cannot be applied to this case. Category II, on the other hand, produces the largest spread, with several models exceeding the allowed range of  $\Lambda_{1.4}$ . Categories III and IV produce values closer to the constraint, but some EoSs yield values of  $\Lambda_{1.4}$  that fall outside the constraint. This figure therefore highlights how the specific choices of transition pressure and energy-density discontinuity affect non-trivially the tidal properties of SSHS.

Now, after presenting details of our results for each category, we compare the  $g$ -mode frequencies,  $f_g$ , across

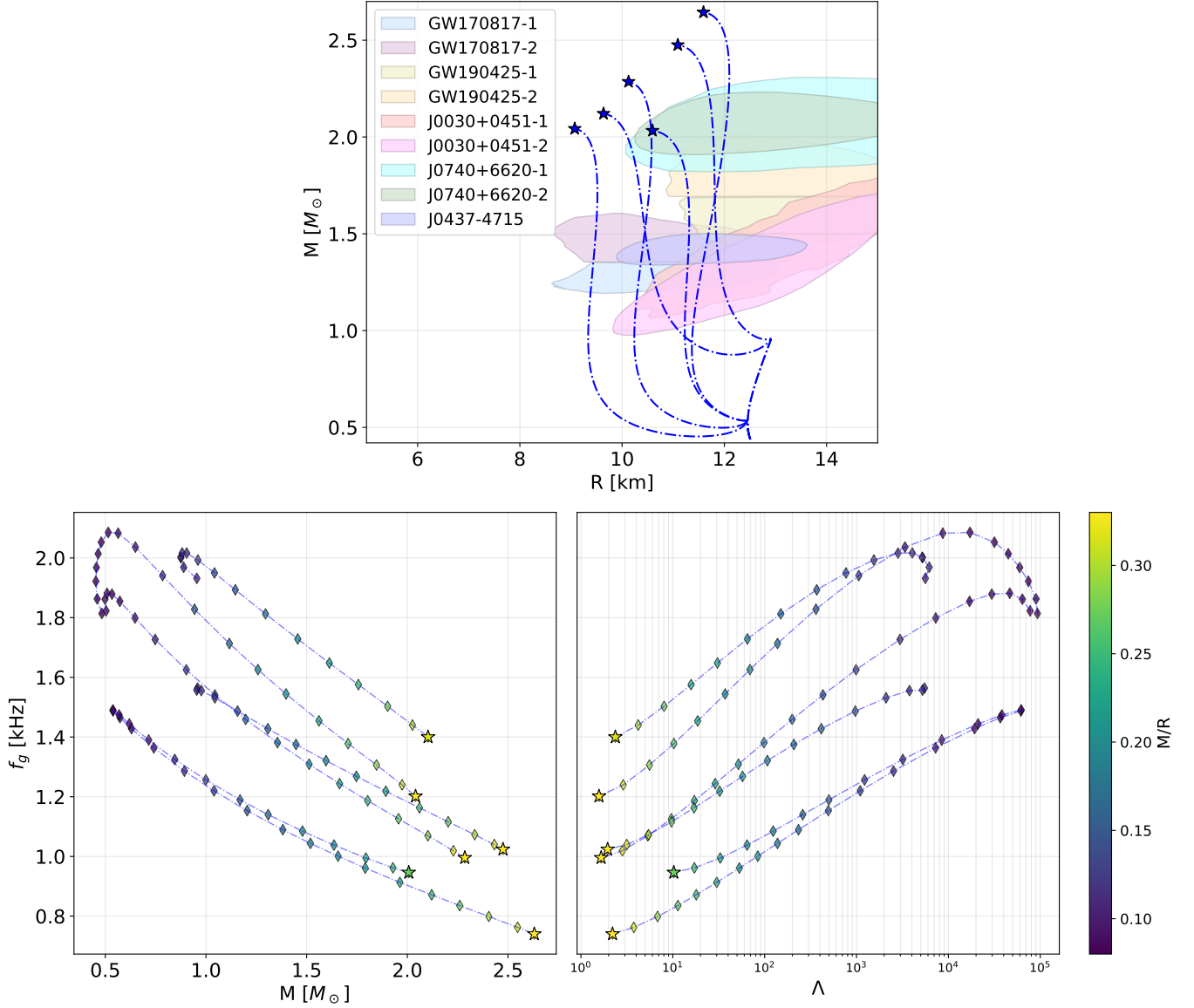


FIG. 5. Results for Category IV twin stars. Same legends and astrophysical constraints as that of Fig. 2.

the different categories in order to probe their qualitative and quantitative differences as a function of the gravitational masses and tidal deformabilities. In Fig. 7, we present these different behaviors for one representative EoS of each category (I–IV). It is revealed in the left panel that Categories I, III, and IV exhibit relatively flat trends, with frequencies between approximately 1.4 and 2.1 kHz across the mass range. In contrast, Category II shows a quite different qualitative and quantitative behavior, with  $f_g$  increasing rapidly for decreasing values of  $M$  and reaching values as high as  $\sim 5$  kHz. We have seen that this novel trend happens because Category II stars have larger  $\Delta\epsilon$  and  $P_t$  that produce such non-trivial behavior compared to the other categories and past works exploring this non-radial mode. This is also manifested in the right panel of Fig. 7 for  $f_g$  against the tidal de-

formabilities where the non-monotonic behavior can be seen. In this sense, one can say that Category II twin stars are the most extreme scenario and potentially the more likely to be detected first due to their high values of  $f_g$  and unique behavior against  $M$  and  $\Lambda$ .

#### IV. UNIVERSAL RELATIONS FOR DISCONTINUITY MODES

We have seen in the previous section that  $g$ -mode frequencies for the four categories are highly sensitive to the sharp energy density jump (or to the energy density jump normalized by the energy density at the transition) at the quark-hadron interface present in the EoSs for twin stars. This motivates us to probe whether a set of universal re-

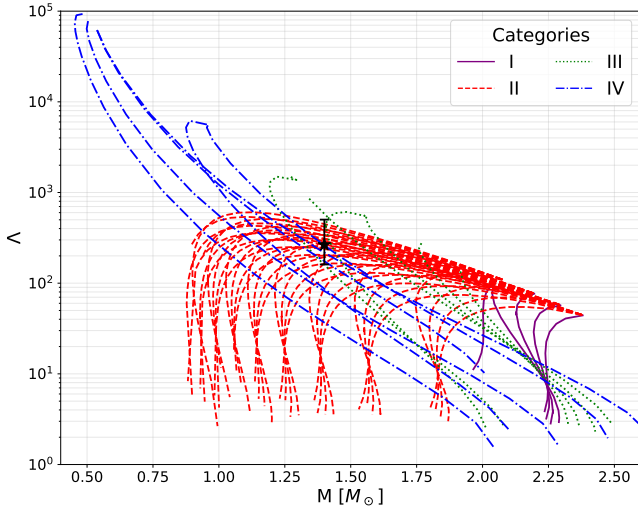


FIG. 6. Dimensionless tidal deformability,  $\Lambda$ , for the SSHS as a function of the gravitational mass,  $M$  for all the categories considered in this work. The colors used are the same as previous figures. We present in black the constraint for the  $\Lambda$  of a  $1.4 M_\odot$  NS obtained in Ref. [83].

lations exists between the frequencies  $f_g$  and  $\Delta\epsilon/\epsilon_{\text{trans}}$  across the wide set of allowed EoSs of Subsec. II A, thus allowing us to classify them by category.

Interestingly, we found that, contrary to what has been proposed in Refs. [33, 52], a relation between the decimal logarithm of  $f_g$  and  $\Delta\epsilon/\epsilon_{\text{trans}}$  does not hold for all EoSs within each category (I–IV). We display these results in Fig. 8 where a trend relating larger values of  $\Delta\epsilon/\epsilon_{\text{trans}}$  to larger values of  $f_g$  appears to exist. Each point corresponds to an individual twin star configuration, color-coded differently for each EoS category. The left panels show the full dataset, while the right panels include a fit for each category using distinct line styles. We performed individual linear fits for a set of EoSs within each category using the function

$$\text{Log}_{10}(f_g) = A + B \text{Log}_{10}(\Delta\epsilon/\epsilon_{\text{trans}}), \quad (10)$$

with the fitting parameters listed in Table II. In addition to the coefficients  $A$  and  $B$  (together with their uncertainties), the table also reports the Pearson correlation coefficient, which measures the strength of the linear relation, and the mean relative error of the fits. The solid gray line corresponds to the relation proposed in Ref. [33], with  $A = 0.255 \pm 0.017$  and  $B = 0.512 \pm 0.022$ , valid for  $\Delta\epsilon/\epsilon_{\text{trans}} \sim 1$ . Our results, however, show low correlation coefficients for most categories. Furthermore, we observe significant deviations from the classical value of  $B = 1/2$ , as reported in Ref. [84].

Due to the lack of universality of the previously proposed relationships, especially when long branches of SSHS are taken into account, it would be interesting to investigate the dependence of the  $g$ -mode frequencies on the features of the phase transition as well as their structural properties. In order to do this, we examine the

Cat.	$A + \sigma_A$	$B + \sigma_B$	Corr. coef.	Rel. error
I	$0.1865 \pm 0.0076$	$0.1200 \pm 0.1110$	0.1339	0.0636
II	$0.3308 \pm 0.0077$	$0.1183 \pm 0.0116$	0.3218	0.1656
III	$0.1980 \pm 0.0033$	$0.5676 \pm 0.0241$	0.9365	0.2076
IV	$0.1298 \pm 0.0090$	$0.4751 \pm 0.0544$	0.6656	3.9867

TABLE II. Fitting parameters  $A$  and  $B$  for Eq. (10) obtained independently for each twin star category, including their uncertainties  $\sigma_A$  and  $\sigma_B$ . The table also reports the Pearson correlation coefficient between the fitted and actual data and the mean relative error of the fit.

potential existence of a unique universal relation, i.e. the same for the four categories of twin stars, that combines  $f_g$ , tidal deformability,  $\Lambda$  and stellar compactness of a canonical NS to the normalized energy density jump. We discovered that such a relation exists, and it is given by:

$$\begin{aligned} \text{Log}_{10} [(f_g/\Lambda_3)(M_{1.4}/R_{10})] = \\ C + D \text{Log}_{10} [(\Delta\epsilon/\epsilon_{\text{trans}})(1/(\Lambda_3^3 R_{10}))], \end{aligned} \quad (11)$$

where  $M_{1.4} \equiv M/1.4 M_\odot$ ,  $R_{10} \equiv R/10$  km, and  $\Lambda_3 \equiv \Lambda/10^3$ . This relationship can be thought of as a generalization of the one presented in Eq. (10) including effects related to macroscopic magnitudes of the compact objects that play a key role, particularly the long branches of SSHS that appear when EoSs of Category II are taken into account. In Fig. 9 we display this novel relationship, where each point corresponds to a stellar configuration from our dataset, being color-coded by EoS category. The dashed black line represents the best linear fit across all categories, with slope  $D = 0.385 \pm 0.001$  and intercept  $C = -0.036 \pm 0.011$ . The high Pearson correlation coefficient (0.9961) indicates a robust universal trend linking  $g$ -mode frequencies to phase transition parameters present in the EoS and global stellar properties. Most points lie within a few percent of the fit, reinforcing the accuracy and predictive power of the proposed universal relation. We close this section by highlighting that our proposed universal relations in this work are the first attempt in the literature to go beyond the usual relations between  $f_g M$  and  $\Lambda$  [85]. These conventional relations do not always produce reliable results approaching the universal curve, often leading to relatively large relative errors compared to those established relations for the  $f$ -mode [85], a mode that is currently under intense research.

## V. SUMMARY AND OUTLOOK

In this work, we explored the quantitative and qualitative behavior of the non-radial  $g$ -mode frequencies (directly associated with the first-order phase transition) for the four categories of twin stars. In order to do this, we used the CSS parametrization of the hybrid EoS to match a hadronic matter phase onto a quark matter phase. The hadronic phase is characterized by a combination of the

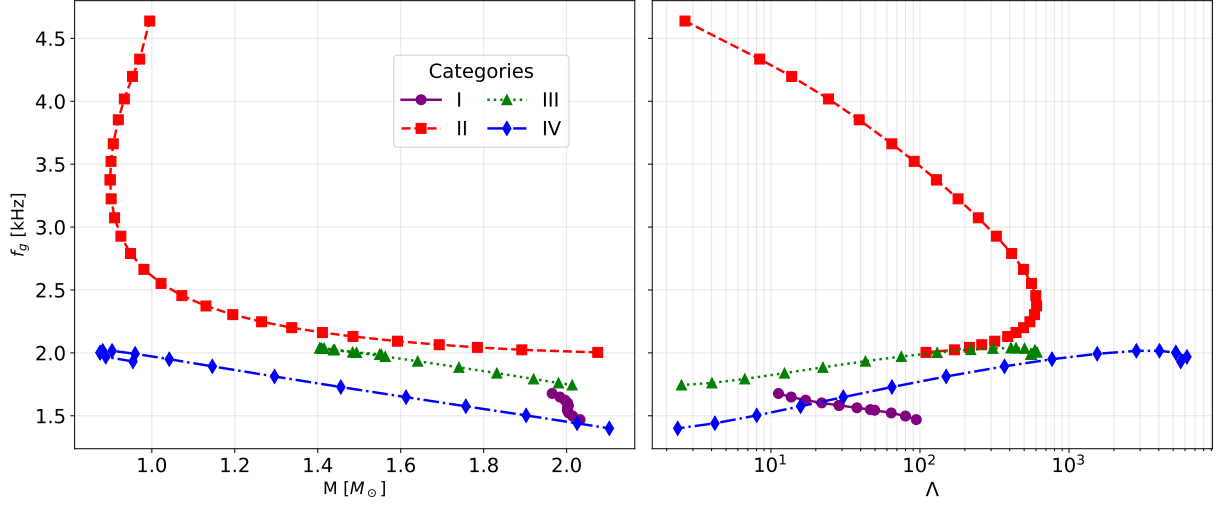


FIG. 7. Comparison of the non-radial  $g$ -mode frequencies,  $f_g$ , as functions of the stellar mass,  $M$ , (left panel) and dimensionless tidal deformabilities,  $\Lambda$ , (right panel), displayed for one representative EoS per twin star category (I–IV). Each one of them is depicted with a distinct line style and marker for clarity.

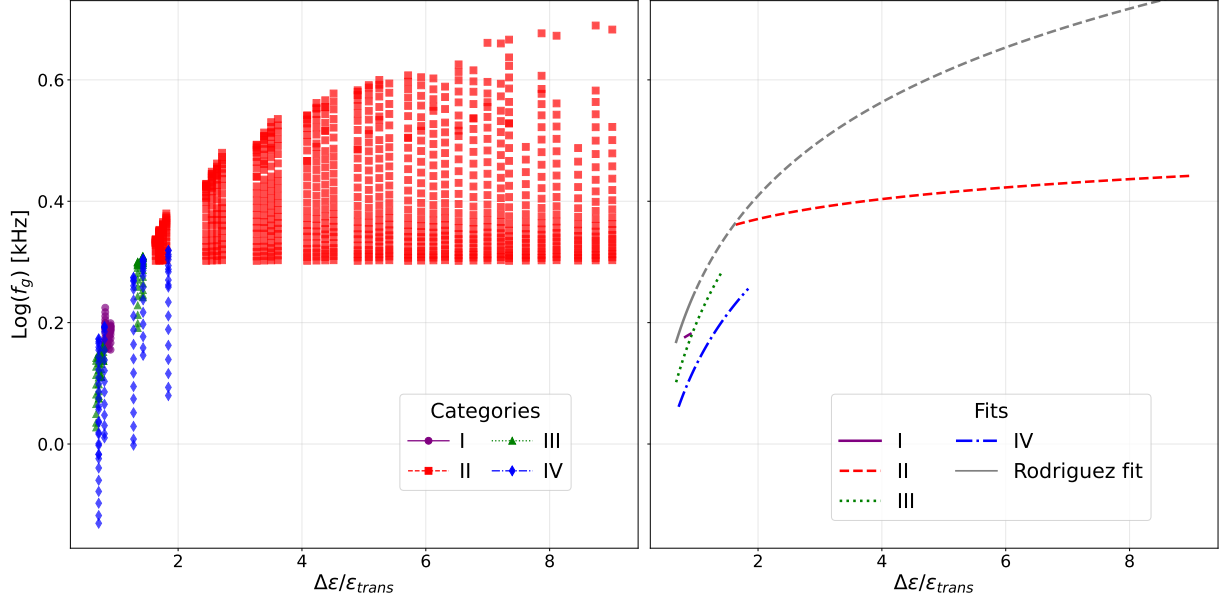


FIG. 8. Relationship between the decimal logarithm of the  $g$ -mode frequencies (in kHz) and the relative energy density variation,  $\Delta\epsilon/\epsilon_{\text{trans}}$ , for all twin star EoSs in each category (I–IV) analyzed in the present work. Points represent individual stellar configurations from our analysis, color-coded by EoS category. The left panel displays the data while the right panel shows their corresponding fit, where different twin star categories are shown with distinct styles. Notice that the right panel also includes (in gray color) the empirical fit (dubbed ‘Rodriguez fit’) proposed in Ref. [33] for comparison. Related to this fit we use continuous line to present original results and, an extrapolation of such fit to larger  $\Delta\epsilon/\epsilon_{\text{trans}}$  with dashed lines.

BPS (at very low densities) and SLy EoS at low baryon densities between  $\sim 0.5 n_0$  and  $1.1 n_0$ , i.e. the region of validity of the CET results. From this density onward, we used three generalized piecewise polytropes (GPP) until the transition point, which, depending on the category of twin stars, is located at different values of  $\{P_t, \Delta\epsilon\}$  and  $c_s^2 \in [0.5, 1]$  of the quark phase. Equipped with these inputs, we solved the TOV equations to obtain the  $M$ - $R$  di-

agrams for each of the four categories of twin stars. Then, applying criteria of Ref. [29] for SSHS, we found that all our stellar families (hadronic and hybrid) branches are dynamically stable against radial oscillations.

These results were employed to solve the relativistic quasi-normal non-radial oscillation equations to determine the  $g$ -mode frequencies,  $f_g$ , in the relativistic Cowling approximation. After careful numerical calculations,



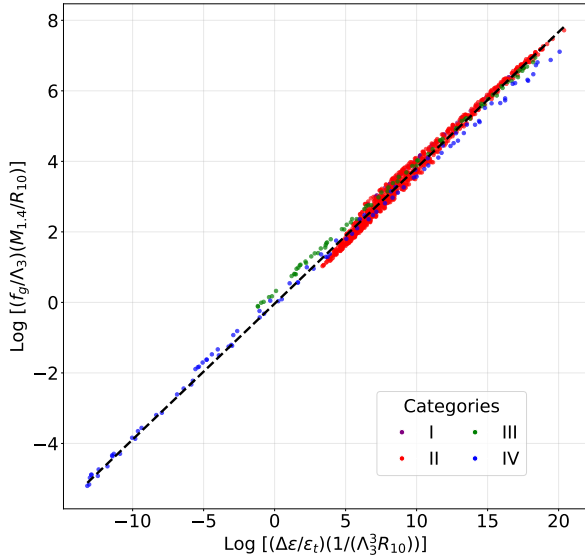


FIG. 9. Proposed novel universal relation for twin stars of Eq. (12). Points represent individual stellar configurations from our analysis, color-coded by EoS category. The dashed black line shows a linear fit to these data, demonstrating a tight correlation across twin star categories.

we found the explicit dependencies of  $f_g$  on the stellar mass,  $M$  and tidal deformability,  $\Lambda$ . Apart from expected quantitative differences for results between categories, strongly related to the triad  $\{P_t, \Delta\epsilon, c_s^2 \in [0.5, 1]\}$ , we discovered a global explanation for their qualitative peculiarities.

We also explored the exciting possibility of building universal relations for: a) each category of HSs and b) a unique formula encompassing the four categories. For a), following the reasoning of Ref. [33], we found four laws that despite having small correlation coefficient, relate  $\text{Log}_{10}(f_g)$  to  $\Delta\epsilon/\epsilon_{\text{trans}}$ . Interestingly, they display notoriously distinct slopes, departing from the 1/2 result obtained with Newtonian gravity. These findings will be useful for future direct or indirect detection of the  $g$ -mode frequencies in hybrid stars (solitary or in binary systems) with strong phase transitions (already knowing that they are twin stars by their behavior in the  $M$ - $R$  diagram) and infer  $\Delta\epsilon/\epsilon_{\text{trans}}$ . For b), based upon our calculations for the  $g$ -mode frequencies of Sec. III, we proposed a logarithmic relation between  $f_g$ , compactness of a canonical NS, normalized energy density jump and tidal deformabilities. This linear formula found unified results for all the categories with very low values of relative error. This gives us confidence to use it to extract information about the phase transition in terms of usually measured values of compactness and tidal deformabilities of NSs. Such relations are, therefore, highly relevant for inferring non-radial frequencies through gravitational wave data, as it was already done for the non-radial  $f$ -mode frequencies [86].

Moreover, if a simultaneous detection of a  $g$ -mode and

the fundamental  $wI$ -mode occurs, the universal relationships from Ref. [40] could be used to constrain the star's mass and radius (within a few percent) and its dimensionless tidal deformability (within a factor of 2). These estimations would then serve to determine  $\Delta\epsilon/\epsilon_{\text{trans}}$  via the universal relationship established in this work.

Of course, to be dealt with, is the question of the detectability (directly or indirectly) of our proposed  $g$ -mode classes (and associated universal relations) from modern and upcoming gravitational wave data.

Firstly, it is interesting to discuss the energetics needed in order to estimate the potential detectability of these  $g$ -mode frequencies of twin stars in future gravitational-wave detectors (like the Advanced LIGO-Virgo and Einstein telescopes). The frequencies of the  $g$ -modes associated with compact configurations of Categories I, III, and IV are comparable to those studied in Refs. [32, 33], for this reason, we expect a similar energy threshold. The situation changes when objects of Category II are taken into account. For this family, the  $g$ -modes span a larger range of frequencies where, in addition, gravitational-wave detectors do not present their best sensitivities. Despite a more detailed analysis is needed, we expect that for these objects, a larger amount of energy has to be channeled into gravitational waves so that they become detectable.

Interestingly, a recent complementary research presented in Ref. [87] pointed out the difficulty of reliably distinguishing  $f$ -mode frequencies from the  $g$ -mode in hybrid stars. This challenge arises from their simultaneous coupling with the dynamical tidal field, producing an overlap between their numerical values for stellar masses from 1.4 to 2  $M_\odot$ . However, they only considered a fixed value of  $P_t$  while making slight variations of the transition jump, i.e.,  $\Delta\epsilon = (1 + P_t/\epsilon_t)\Delta n_B/n_t$  maximally reaching values around 1. However, we believe that a similar study must be carried out considering strong first-order phase transitions for which we have seen that the  $g$ -mode frequencies behave quite differently (quantitatively and qualitatively) for the four categories of twin stars, something that is out of the scope of the present work and is left as future work.

## ACKNOWLEDGMENTS

M.C.R is a doctoral fellow at CONICET (Argentina). M.C.R and I.F.R-S. acknowledge UNLP and CONICET (Argentina) for financial support under grants G187 and PIP 0169. J.C.J. is supported by Conselho Nacional de Desenvolvimento Científico e Tecnológico (CNPq) with Grant No. 151390/2024-0. The work of I.F.R-S. was also partially supported by PIBAA 0724 from CONICET.

### Appendix A: Explicit solutions for the $g$ -modes of the $V$ and $W$ eigenfunctions

Radial profiles of the eigenfunctions  $V$  and  $W$  for the  $g$ -mode are shown in Fig. 10, calculated for stellar configurations representative of Categories I through IV. Each curve is normalized by its respective maximum amplitude, i.e.  $\tilde{V}$  and  $\tilde{W}$ , and consistent colors are used to represent both eigenfunctions within each category. The discontinuity observed in the  $\tilde{V}$  eigenfunction occurs at the hadron-quark phase transition in the core of the star. Similarly, the eigenfunction  $\tilde{W}$  exhibits an abrupt change in its radial derivative at the location of the phase transition. Notably, in all cases, both eigenfunctions present a single node in their radial profiles, confirming the classification of the mode as a  $g$ -mode or  $p$ -mode according to the Cowling classification scheme. Given that the frequencies are lower than the ones of the node-less  $f$ -mode, we identify them as  $g$ -modes within the Cowling framework.

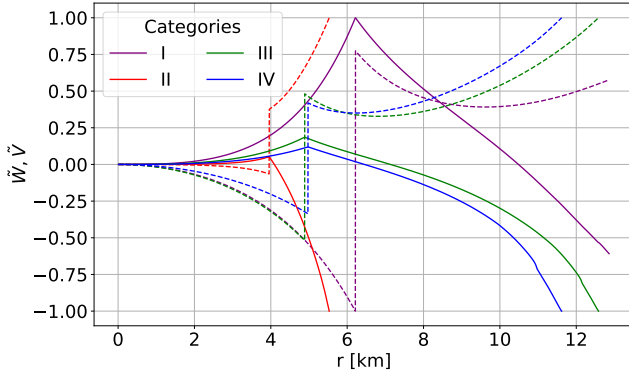


FIG. 10. Radial profiles of the normalized (by their respective maximum amplitudes) eigenfunctions  $\tilde{W}(r)$  (solid lines) and  $\tilde{V}(r)$  (dashed lines) for the  $g$ -mode, computed for stellar configurations representative of Categories I-IV. The same color is used for both eigenfunctions within each category.

### Appendix B: Tidal deformability in neutron stars with a first-order phase transition

The calculation of the dimensionless tidal deformability,  $\Lambda$ , follows the formalism outlined below. For

quadrupolar perturbations,  $\Lambda$  is related to the Love number,  $k_2$ , which can be obtained by solving, together with the TOV equations, an additional differential equation:

$$r \frac{d\zeta(r)}{dr} + \zeta(r)^2 + \zeta(r) \frac{1 + 4\pi r^2 [P(r) + \epsilon(r)]}{1 - \frac{2m(r)}{r}} - \frac{6 - 4\pi r^2 \left[ 5\epsilon(r) + 9P(r) + \frac{\epsilon(r) + P(r)}{dP/d\epsilon} \right]}{1 - \frac{2m(r)}{r}} - \left( r \frac{d\nu(r)}{dr} \right)^2 = 0, \quad (\text{B1})$$

with the boundary condition  $\zeta(0) = 2$ . Furthermore, for EoSs with abrupt discontinuities at radii  $r = r_t$ , the additional matching condition

$$\zeta(r_t^+) - \zeta(r_t^-) = \frac{4\pi r_t^3 [\epsilon(r_t^+) - \epsilon(r_t^-)]}{m(r_t) + 4\pi(r_t)^3 P(r_t)}, \quad (\text{B2})$$

must be imposed [88, 89]. The superscripts  $+$  and  $-$  represent the values at the transition radius on either side of the interface. After solving Equation (B1), we compute the Love number,  $k_2$ , using the following expression,

$$k_2 = \frac{8}{5} \beta^5 (1 - 2\beta)^2 [2 + 2\beta(\zeta - 1) - \zeta] \times \left[ 2\beta[6 - 3\zeta + 3\beta(5\zeta - 8)] + 4\beta^3[13 - 11\zeta + \beta(3\zeta - 2) + 2\beta^2(\zeta + 1)] + 3(1 - 2\beta)^2[2 - \zeta + 2\beta(\zeta - 1)] \ln(1 - 2\beta) \right]^{-1}, \quad (\text{B3})$$

where  $\zeta \equiv \zeta(R)$ . The quantity  $\beta = M/R$  denotes compactness. The dimensionless tidal deformability is then obtained using the following expression,

$$\Lambda = \frac{2}{3} k_2 \left( \frac{R}{M} \right)^5. \quad (\text{B4})$$

- 
- [1] N. Glendenning, *Compact Stars: Nuclear Physics, Particle Physics and General Relativity*, Astronomy and Astrophysics Library (Springer New York, 2012).
  - [2] J. M. Lattimer and M. Prakash, The physics of neutron stars, *science* **304**, 536 (2004).
  - [3] A. Y. Potekhin, The physics of neutron stars, *Physics-Uspekhi* **53**, 1235 (2010).

- [4] G. Baym *et al.*, From hadrons to quarks in neutron stars: a review, *Reports on Progress in Physics* **81**, 056902 (2018).
- [5] M. G. Orsaria *et al.*, Phase transitions in neutron stars and their links to gravitational waves, *Journal of Physics G: Nuclear and Particle Physics* **46**, 073002 (2019).
- [6] C. Drischler *et al.*, How Well Do We Know the Neutron-Matter Equation of State at the Densities Inside Neu-

- tron Stars? A Bayesian Approach with Correlated Uncertainties, *Phys. Rev. Lett.* **125**, 202702 (2020), [arXiv:2004.07232 \[nucl-th\]](#).
- [7] F. Weber, Strange quark matter and compact stars, *Progress in Particle and Nuclear Physics* **54**, 193 (2005).
- [8] P. B. Demorest, T. Pennucci, S. M. Ransom, M. S. E. Roberts, and J. W. T. Hessels, A two-solar-mass neutron star measured using Shapiro delay, *Nature (London)* **467**, 1081 (2010), [arXiv:1010.5788 \[astro-ph.HE\]](#).
- [9] Z. Arzoumanian *et al.*, The nanograv 11-year data set: high-precision timing of 45 millisecond pulsars, *The Astrophysical Journal Supplement Series* **235**, 37 (2018).
- [10] J. Antoniadis *et al.*, A massive pulsar in a compact relativistic binary, *Science* **340**, 1233232 (2013).
- [11] H. T. Cromartie *et al.*, Relativistic shapiro delay measurements of an extremely massive millisecond pulsar, *Nature Astronomy* **4**, 72 (2020).
- [12] B. P. Abbott *et al.*, Gravitational waves and gamma-rays from a binary neutron star merger: Gw170817 and grb 170817a, *The Astrophysical Journal Letters* **848**, L13 (2017).
- [13] B. P. Abbott *et al.*, Gw170817: Measurements of neutron star radii and equation of state, *Physical review letters* **121**, 161101 (2018).
- [14] B. P. Abbott *et al.*, Gw190425: Observation of a compact binary coalescence with total mass  $\sim 3.4m_{\odot}$ , *The Astrophysical Journal* **892**, L3 (2020).
- [15] M. Miller *et al.*, Psr j0030+ 0451 mass and radius from nicer data and implications for the properties of neutron star matter, *The Astrophysical Journal Letters* **887**, L24 (2019).
- [16] T. E. Riley *et al.*, A nicer view of psr j0030+ 0451: millisecond pulsar parameter estimation, *The Astrophysical Journal Letters* **887**, L21 (2019).
- [17] M. C. Miller *et al.*, The radius of psr j0740+ 6620 from nicer and xmm-newton data, *The Astrophysical Journal Letters* **918**, L28 (2021).
- [18] T. E. Riley *et al.*, A nicer view of the massive pulsar psr j0740+ 6620 informed by radio timing and xmm-newton spectroscopy, *The Astrophysical Journal Letters* **918**, L27 (2021).
- [19] T. Salmi *et al.*, The radius of the high-mass pulsar psr j0740+ 6620 with 3.6 yr of nicer data, *The Astrophysical Journal* **974**, 294 (2024).
- [20] D. Choudhury *et al.*, A nicer view of the nearest and brightest millisecond pulsar: Psr j0437–4715, *The Astrophysical Journal Letters* **971**, L20 (2024).
- [21] M. Troyer and U.-J. Wiese, Computational complexity and fundamental limitations to fermionic quantum monte carlo simulations, *Phys. Rev. Lett.* **94**, 170201 (2005).
- [22] G. Pan and Z. Y. Meng, The sign problem in quantum monte carlo simulations, in *Encyclopedia of Condensed Matter Physics (Second Edition)* (Academic Press, Oxford, 2024) pp. 879–893.
- [23] L. S. Finn, g-modes of non-radially pulsating relativistic stars: the slow-motion formalism, *Monthly Notices of the Royal Astronomical Society* **222**, 393 (1986).
- [24] L. S. Finn, g-modes in zero-temperature neutron stars, *Monthly Notices of the Royal Astronomical Society* **227**, 265 (1987).
- [25] L. S. Finn, Relativistic stellar pulsations in the cowling approximation, *Monthly Notices of the Royal Astronomical Society* **232**, 259 (1988).
- [26] O. Komoltsev, First-order phase transitions in the cores of neutron stars, *Phys. Rev. D* **110**, L071502 (2024), [arXiv:2404.05637 \[nucl-th\]](#).
- [27] C. Ecker *et al.*, Locating the QCD critical point with neutron-star observations, *arXiv e-prints* **10.48550/arXiv.2506.10065** (2025).
- [28] G. Lugones and A. G. Grunfeld, Phase conversions in neutron stars: Implications for stellar stability and gravitational wave astrophysics, *Universe* **7**, 493 (2021).
- [29] J. P. Pereira, C. V. Flores, and G. Lugones, Phase transition effects on the dynamical stability of hybrid neutron stars, *The Astrophysical Journal* **860**, 12 (2018).
- [30] M. Mariani *et al.*, Magnetized hybrid stars: effects of slow and rapid phase transitions at the quark–hadron interface, *MNRAS* **489**, 4261 (2019).
- [31] G. Malfatti, M. G. Orsaria, I. F. Ranea-Sandoval, G. A. Contrera, and F. Weber, Delta baryons and diquark formation in the cores of neutron stars, *Physical Review D* **102**, 063008 (2020).
- [32] L. Tonetto and G. Lugones, Discontinuity gravity modes in hybrid stars: Assessing the role of rapid and slow phase conversions, *Physical Review D* **101**, 123029 (2020).
- [33] M. C. Rodríguez *et al.*, Hybrid stars with sequential phase transitions: the emergence of the  $g_2$  mode, *JCAP* **2021** (2), 009, [arXiv:2009.03769 \[astro-ph.HE\]](#).
- [34] D. Curin, I. F. Ranea-Sandoval, M. Mariani, M. G. Orsaria, and F. Weber, Hybrid stars with color superconducting cores in an extended fcm model, *Universe* **7**, 370 (2021).
- [35] V. P. Gonçalves and L. Lazzari, Impact of slow conversions on hybrid stars with sequential qcd phase transitions, *The European Physical Journal C* **82**, 288 (2022).
- [36] M. Mariani *et al.*, Oscillating magnetized hybrid stars under the magnifying glass of multimessenger observations, *MNRAS* **512**, 517 (2022).
- [37] I. F. Ranea-Sandoval *et al.*, Breaking of universal relationships of axial  $w_i$  modes in hybrid stars: Rapid and slow hadron-quark conversion scenarios, *Physical Review D* **106**, 043025 (2022).
- [38] G. Lugones, M. Mariani, and I. F. Ranea-Sandoval, A model-agnostic analysis of hybrid stars with reactive interfaces, *Journal of Cosmology and Astroparticle Physics* **2023** (03), 028.
- [39] I. F. Ranea-Sandoval *et al.*, Asteroseismology using quadrupolar f-modes revisited: Breaking of universal relationships in the slow hadron-quark conversion scenario, *Physical Review D* **107**, 123028 (2023).
- [40] I. F. Ranea-Sandoval *et al.*, Constraining mass, radius, and tidal deformability of compact stars with axial  $w_i$  modes: new universal relations including slow stable hybrid stars, *MNRAS* **519**, 3194 (2023).
- [41] P. B. Rau and A. Sedrakian, Two first-order phase transitions in hybrid compact stars: Higher-order multiplet stars, reaction modes, and intermediate conversion speeds, *Physical Review D* **107**, 103042 (2023).
- [42] P. B. Rau and G. G. Salaben, Nonequilibrium effects on stability of hybrid stars with first-order phase transitions, *Phys. Rev. D* **108**, 103035 (2023), [arXiv:2309.08540 \[astro-ph.HE\]](#).
- [43] I. A. Rather *et al.*, Radial oscillations of hybrid stars and neutron stars including delta baryons: the effect of a slow quark phase transition, *Journal of Cosmology and Astroparticle Physics* **2024** (05), 130.

- [44] J. C. Jiménez, L. Lazzari, and V. P. Gonçalves, How the qcd trace anomaly behaves at the core of twin stars?, *Physical Review D* **110**, 114014 (2024).
- [45] P. Laskos-Patkos and C. C. Moustakidis, Xte j1814-338: A potential hybrid star candidate, *Physical Review D* **111**, 063058 (2025).
- [46] P. D. Lasky, Gravitational waves from neutron stars: a review, *Publications of the Astronomical Society of Australia* **32**, e034 (2015).
- [47] B. Haskell and K. Schwenzer, Isolated neutron stars, in *Handbook of Gravitational Wave Astronomy* (Springer, 2022) pp. 527–554.
- [48] N. Andersson, A gravitational-wave perspective on neutron-star seismology, *Universe* **7**, 97 (2021).
- [49] J. A. Font, Gravitational Waves from Neutron Stars: Detection Prospects and Inferences for Two Distinct Types of Remnants, *Acta Phys. Polon. B* **56**, 5 (2025).
- [50] H. Sotani, K. Tominaga, and K.-i. Maeda, Density discontinuity of a neutron star and gravitational waves, *Physical Review D* **65**, 024010 (2001).
- [51] C. Vásquez Flores and G. Lugones, Discriminating hadronic and quark stars through gravitational waves of fluid pulsation modes, *Classical and Quantum Gravity* **31**, 155002 (2014).
- [52] I. F. Ranea-Sandoval *et al.*, Oscillation modes of hybrid stars within the relativistic cowling approximation, *JCAP* **2018** (12), 031.
- [53] T. Zhao *et al.*, Suppression of composition g-modes in chemically-equilibrating warm neutron stars, *arXiv preprint arXiv:2504.12230* (2025).
- [54] N. Andersson and K. D. Kokkotas, Towards gravitational wave asteroseismology, *MNRAS* **299**, 1059 (1998), [arXiv:gr-qc/9711088 \[gr-qc\]](#).
- [55] O. Benhar, V. Ferrari, and L. Gualtieri, Gravitational wave asteroseismology reexamined, *Phys.Rev.D* **70**, 124015 (2004), [arXiv:astro-ph/0407529 \[astro-ph\]](#).
- [56] L. K. Tsui and P. T. Leung, Universality in quasi-normal modes of neutron stars, *MNRAS* **357**, 1029 (2005), [arXiv:gr-qc/0412024 \[gr-qc\]](#).
- [57] C. Chirenti *et al.*, Fundamental oscillation modes of neutron stars: Validity of universal relations, *Phys.Rev.D* **91**, 044034 (2015), [arXiv:1501.02970 \[gr-qc\]](#).
- [58] H. K. Lau *et al.*, Inferring Physical Parameters of Compact Stars from their f-mode Gravitational Wave Signals, *ApJ* **714**, 1234 (2010), [arXiv:0911.0131 \[gr-qc\]](#).
- [59] H. Sotani and B. Kumar, Universal relations between the quasinormal modes of neutron star and tidal deformability, *Phys.Rev.D* **104**, 123002 (2021).
- [60] B. K. Pradhan *et al.*, Probing hadron–quark phase transition in twin stars using f-modes, *Monthly Notices of the Royal Astronomical Society* **531**, 4640 (2024).
- [61] J. L. Blázquez-Salcedo *et al.*, Phenomenological relations for axial quasinormal modes of neutron stars with realistic equations of state, *Phys. Rev. D* **87**, 104042 (2013).
- [62] A. Guha, D. Sen, and C. H. Hyun, Non-radial oscillations of hadronic neutron stars, quark stars, and hybrid stars: calculation of f, p, and g mode frequencies, *Eur. Phys. J. C* **85**, 442 (2025), [arXiv:2412.18569 \[hep-ph\]](#).
- [63] U. H. Gerlach, Equation of State at Supranuclear Densities and the Existence of a Third Family of Superdense Stars, *Phys. Rev.* **172**, 1325 (1968).
- [64] K. Schertler *et al.*, Quark phases in neutron stars and a ‘third family’ of compact stars as a signature for phase transitions, *Nucl. Phys. A* **677**, 463 (2000), [arXiv:astro-ph/0001467](#).
- [65] D. E. Alvarez-Castillo and D. B. Blaschke, High-mass twin stars with a multipolytrope equation of state, *Phys. Rev. C* **96**, 045809 (2017), [arXiv:1703.02681 \[nucl-th\]](#).
- [66] J.-E. Christian *et al.*, Classifications of Twin Star Solutions for a Constant Speed of Sound Parameterized Equation of State, *Eur. Phys. J. A* **54**, 28 (2018), [arXiv:1707.07524 \[astro-ph.HE\]](#).
- [67] J.-E. Christian *et al.*, Which first order phase transitions to quark matter are possible in neutron stars?, *Phys. Rev. D* **109**, 063035 (2024), [arXiv:2312.10148 \[nucl-th\]](#).
- [68] N. K. Glendenning and C. Kettner, Nonidentical neutron star twins, *Astron. Astrophys.* **353**, L9 (2000), [arXiv:astro-ph/9807155](#).
- [69] W. Wei *et al.*, Lifting the Veil on Quark Matter in Compact Stars with Core g-mode Oscillations, *Astrophys. J.* **904**, 187 (2020), [arXiv:1811.11377 \[nucl-th\]](#).
- [70] P. Jaikumar *et al.*, g-mode oscillations in hybrid stars: A tale of two sounds, *Phys. Rev. D* **103**, 123009 (2021), [arXiv:2101.06349 \[nucl-th\]](#).
- [71] C. Constantinou *et al.*, g modes of neutron stars with hadron-to-quark crossover transitions, *Phys. Rev. D* **104**, 123032 (2021), [arXiv:2109.14091 \[astro-ph.HE\]](#).
- [72] T. Zhao, C. Constantinou, P. Jaikumar, and M. Prakash, Quasinormal g modes of neutron stars with quarks, *Phys. Rev. D* **105**, 103025 (2022), [arXiv:2202.01403 \[gr-qc\]](#).
- [73] D. Kumar, H. Mishra, and T. Malik, Non-radial oscillation modes in hybrid stars: consequences of a mixed phase, *Journal of Cosmology and Astroparticle Physics* **2023** (2), 015, [arXiv:2110.00324 \[hep-ph\]](#).
- [74] F. Gittins and N. Andersson, Neutron-star seismology with realistic, finite-temperature nuclear matter, *Phys. Rev. D* **111**, 083024 (2025), [arXiv:2406.05177 \[gr-qc\]](#).
- [75] M. G. Alford, S. Han, M. Prakash, *et al.*, Generic conditions for stable hybrid stars, *Physical Review D* **88**, 083013 (2013).
- [76] F. Douchin and P. Haensel, A unified equation of state of dense matter and neutron star structure, *Astron. Astrophys.* **380**, 151 (2001), [arXiv:astro-ph/0111092](#).
- [77] K. Hebeler *et al.*, Equation of state and neutron star properties constrained by nuclear physics and observation, *Astrophys. J.* **773**, 11 (2013), [arXiv:1303.4662 \[astro-ph.SR\]](#).
- [78] G. Baym *et al.*, The ground state of matter at high densities: equation of state and stellar models, *Astrophysical Journal*, vol. 170, p. 299 **170**, 299 (1971).
- [79] L. S. Finn, Relativistic stellar pulsations in the cowling approximation, *Monthly Notices of the Royal Astronomical Society* **232**, 259 (1988).
- [80] H. Sotani *et al.*, Signatures of hadron-quark mixed phase in gravitational waves, *Physical Review D—Particles, Fields, Gravitation, and Cosmology* **83**, 024014 (2011).
- [81] B. P. Abbott *et al.* (LIGO Scientific Collaboration and Virgo Collaboration), GW170817: Observation of Gravitational Waves from a Binary Neutron Star Inspiral, *Phys. Rev. Lett.* **119**, 161101 (2017).
- [82] A. Guha, D. Sen, and C. H. Hyun, Non-radial oscillations of hadronic neutron stars, quark stars, and hybrid stars: calculation of f, p, and g mode frequencies, *European Physical Journal C* **85**, 442 (2025), [arXiv:2412.18569 \[hep-ph\]](#).
- [83] C. Huang, Model-independent Determination of the Tidal Deformability of a 1.4  $M_{\odot}$  Neutron Star from Gravitational-wave Measurements, *Astrophys. J.* **985**,



- 216 (2025), [arXiv:2505.14822 \[astro-ph.HE\]](#).
- [84] P. N. McDermott, Density Discontinuity G-Modes, *Monthly Notices of the Royal Astronomical Society* **245**, 508 (1990).
  - [85] H.-J. Kuan *et al.*, Constraining equation-of-state groups from g-mode asteroseismology, *Mon. Not. Roy. Astron. Soc.* **513**, 4045 (2022), [arXiv:2204.08492 \[gr-qc\]](#).
  - [86] G. Pratten, P. Schmidt, and T. Hinderer, Gravitational-Wave Asteroseismology with Fundamental Modes from Compact Binary Inspirals, *Nature Commun.* **11**, 2553 (2020), [arXiv:1905.00817 \[gr-qc\]](#).
  - [87] J. P. Pereira *et al.*, Dynamical tides in neutron stars with first-order phase transitions: the role of the discontinuity mode, *arXiv e-prints* [10.48550/arXiv.2504.16911](#) (2025).
  - [88] J. Takátsy and P. Kovács, Comment on “Tidal Love numbers of neutron and self-bound quark stars”, *Phys. Rev. D* **102**, 028501 (2020), [arXiv:2007.01139 \[astro-ph.HE\]](#).
  - [89] S. Han and A. W. Steiner, Tidal deformability with sharp phase transitions in binary neutron stars, *Phys. Rev. D* **99**, 083014 (2019), [arXiv:1810.10967 \[nucl-th\]](#).